World Journal of Biological Chemistry

Online Submissions: http://www.wjgnet.com/1949-8454office
wjbc@wjgnet.com
doi:10.4331/wjbc.v2.i5.90

World J Biol Chem 2011 May 26; 2(5): 90-97
ISSN 1949-8454 (online)

ORIGINAL ARTICLE

High tolerance to mutations in a *Chlamydia trachomatis* peptide deformylase loop

Christopher B Oey, Xiaofeng Bao, Christal Lewis, John E Kerrigan, Huizhou Fan

Christopher B Oey, Xiaofeng Bao, Christal Lewis, Huizhou Fan, Department of Physiology and Biophysics, Robert Wood Johnson Medical School, University of Medicine and Dentistry of New Jersey, Piscataway, NJ 08854, United States
John E Kerrigan, Cancer Institute of New Jersey, Robert Wood Johnson Medical School, University of Medicine and Dentistry of New Jersey, Piscataway, New Brunswick, NJ 08903, United States
Author contributions: Oey CB and Bao X made equal contributions to this work; Fan H and Kerrigan JE designed the study; Oey CB, Bao X, Lewis C and Kerrigan JE performed the experiments; Fan H and Kerrigan JE analyzed the data and wrote the manuscript.
Supported by A grant from the National Institutes of Health (AI071954) to Fan H
Correspondence to: Huizhou Fan, MD, PhD, Department of Physiology and Biophysics, Robert Wood Johnson Medical School, University of Medicine and Dentistry of New Jersey, 683 Hoes Lane, Piscataway, NJ 08854, United States. fanhu@umdnj.edu
Telephone: +1-732-2354607 Fax: +1-732-2355038
Received: April 9, 2011 Revised: April 27, 2011
Accepted: May 4, 2011
Published online: May 26, 2011

Abstract

AIM: To determine if and how a loop region in the peptide deformylase (PDF) of *Chlamydia trachomatis* regulates enzyme function.

METHODS: Molecular dynamics simulation was used to study a structural model of the chlamydial PDF (cPDF) and predict the temperature factor per residue for the protein backbone atoms. Site-directed mutagenesis was performed to construct cPDF variants. Catalytic properties of the resulting variants were determined by an enzyme assay using formyl-Met-Ala-Ser as a substrate.

RESULTS: *In silico* analysis predicted a significant increase in atomic motion in the DGELV sequence (residues 68-72) of a loop region in a cPDF mutant, which is resistant to PDF inhibitors due to two amino acid substitutions near the active site, as compared to wild-type cPDF. The D68R and D68R/E70R cPDF variants demonstrated significantly increased catalytic efficiency. The E70R mutant showed only slightly decreased efficiency. Although deletion of residues 68-72 resulted in a nearly threefold loss in substrate binding, this deficiency was compensated for by increased catalytic efficiency.

CONCLUSION: Movement of the DGELV loop region is involved in a rate-limiting conformational change of the enzyme during catalysis. However, there is no stringent sequence requirement for this region for cPDF enzyme activity.

Key words: Antibacterial; *Chlamydia*; Peptide deformylase; Sexually transmitted infection

Peer reviewers: Gerardo Corzo, PhD, Department of Molecular Medicine and Bioprocess, Instituto de Biotecnología /UNAM, Av. Universidad #2001, Col. Chamilpa C.P. 62210, Cuernavaca, Morelos, Mexico; Andrea Trabocchi, PhD, Department of Chemistry "Ugo Schiff", University of Florence, Via della Lastruccia 13, I-50019, Sesto Fiorentino, Florence, Italy

Oey CB, Bao X, Lewis C, Kerrigan JE, Fan H. High tolerance to mutations in a *Chlamydia trachomatis* peptide deformylase loop. *World J Biol Chem* 2011; 2(5): 90-97 Available from: URL: http://www.wjgnet.com/1949-8454/full/v2/i5/90.htm DOI: http://dx.doi.org/10.4331/wjbc.v2.i5.90

INTRODUCTION

Bacterial infection is a leading cause of death worldwide. Bacteria are increasingly resistant to antibiotics, but few new antibiotics have been developed in the past 3-4 decades. As a result, the number of effective antibiotic

pipelines for several infectious diseases has now been reduced to one or two. This underscores the importance of identification and characterization of potential new antibacterial targets.

The protein sequence of newly synthesized bacterial proteins starts with an *N*-formyl methionine. Sequential removal of the *N*-formyl group and methionine residue by peptide deformylase (PDF) and *N*-methionine peptidase is essential for either maturation into functional proteins or the degradation of functional formylated proteins as required for bacterial survival[1]. Studies have shown that PDF is a promising therapeutic target of a variety of bacterial pathogens. Accordingly, there have been tremendous efforts to develop new antibiotics that target PDF[2,3].

Conceptually, two types of PDF inhibitors can be therapeutically useful. The first type is broad spectrum inhibitors that are effective against a large variety of pathogens. Most (if not all) PDF inhibitors developed to date fall into this category since they are pseudosubstrate-based compounds[3,4]. Although the PDF proteins from different bacteria share relatively low homology, they have a conserved tertiary structure[5-8]. As a result, pseudosubstrate-based inhibitors, either naturally occurring or developed for the PDF from a specific species, can also inhibit the enzyme from multiple species. However, for the prevention and treatment of certain infections, narrow-spectral PDF inhibitors that target specific pathogens may be more desirable. For example, successful treatment of tuberculosis requires months of medication, therefore, highly specific anti-mycobacterials would minimize the risk of normal microflora disruption and the selection of resistant strains in other species. Furthermore, specific mycobacterial PDF (mPDF) inhibitors may also reduce host cell toxicity because mammals, including humans, also encode a PDF (although the function of this enzyme is not well understood). Interestingly, mPDF contains three consecutive Arg residues in a loop region, which is unique among all PDFs examined. It has been shown that mutation of the Arg residues significantly reduces the catalytic properties of mPDF[9]. Therefore, this mPDF loop is a potential specific anti-tuberculosis target.

Sexually transmitted infection is another highly challenging health problem. *Chlamydia trachomatis* (*C. trachomatis*) is a leading sexually transmitted pathogen. Most patients with *C. trachomatis* infection exhibit only mild or even no symptoms, therefore, they do not seek medical treatment. However, a significant proportion of the untreated patients develop severe complications such as pelvic inflammatory disease and infertility[10]. In the absence of an effective vaccine, chemopreventive measures are being sought after. Since re-infection is very common, as a result of the existence of multiple *C. trachomatis* serovars and the inability of the human body to mount lasting protective immunity against the pathogens, chemoprevention needs to be implemented among the sexually active population as long as they practice unprotected sex. For this reason, only antichlamydials with little or no effects on other microbial species and the human host should be used for the prevention of sexually transmitted chlamydial infection.

PDF is also essential for *C. trachomatis*. PDF inhibitors effectively inhibit chlamydial replication not only in cell culture, but also in a genital infection mouse model, suggesting that chlamydial PDF (cPDF) is a potential prophylactic and therapeutic target[11,12]. In characterizing a cPDF variant, we found that mutation of two amino acids resulted in a significant increase in atomic motion in the loop region corresponding to the mPDF loop region that contained the three critical Arg residues. However, our analysis showed that radical substitutions in the cPDF loop region either had little effect on enzyme kinetics or resulted in improved catalytic efficiency, indicating high sequence flexibility in the enzyme.

MATERIALS AND METHODS

In silico structural modeling

All graphics/workstation-level computations were performed on a Sun Ultra 24 Linux workstation. Graphical illustrations were prepared using the VMD program[13]. A multiple template approach was used to build a homology model of *C. trachomatis* PDF using the Modeller (9v5) program[14]. The following PDF structures were used as templates: 1RL4A of *Plasmodium falciparum*[15]; 1XEOA of *Escherichia coli* (*E. coli*)[16]; 1N5NA of *Thermus thermophilus*[6]; and 1V3YA of *Pseudomonas aeruginosa*[17]. Results of alignment of amino acid sequences of these proteins with cPDF are shown in Figure 1. All of these templates have a sequence identity to cPDF of 42% or higher. The high-energy loop region (residues 61-76) was refined using the loop refinement algorithm in Modeller. The Procheck program[18] was used for stereochemical analysis of the model. The Ramachandran plot analysis of the final lowest energy model revealed that 99.4% of residues were in core or allowable regions (Figure 2). The G-factor analysis revealed no unusual dihedrals or other properties.

The Amber 10 suite of biomolecular simulation programs was used for all molecular dynamics calculations and results analysis[19]. All molecular dynamics computations were performed on the Ranger supercomputer at the Texas Advanced Computer Center, University of Texas at Austin. The force field of Duan *et al*[20] was used to model the proteins for all molecular mechanics calculations. The cationic dummy atom approach was used to model the tetrahedral metal ion in the active site of the enzyme[21,22]. The initial models were energy minimized *in vacuo* to remove bad steric contacts. The model was solvated in a truncated octahedral periodic box of SPC/E water[23], with the overall charge of the system neutralized by insertion of the appropriate number of sodium ions. A 1-nm short-range cutoff was used for all computations. Long-range electrostatics in the model were treated using the particle mesh Ewald method[24,25]. Each system was subjected to energy minimization of the solvent only, followed by minimization of the entire system before dynamics. A 2-fs time step was used for all molecular dy-

```
_aln.pos          10         20         30         40         50         60
1RL4A      ----KIVKYPDPILRRRSEEVTNFDDNLKRVVRKMFDIMYESKGIGLSAPQVNISKRIIVWN------
1XEOA      -SVLQVLHIPDERLRKVAKPVEEVNAEIQRIVDDMFETMYAEEGIGLAATQVDIHQRIIVIDVS-ENR
1N5NA      MAILNILEFPDPRLRTIAKPVEVVDDAVRQLIDDMFETMYEAPGIGLAATQVNVHKRIVVMDLS-EDK
1V3YA      -MVYPIRLYGDPVLRRKARPVEDFS-GIKRLAEDMLETMFEAKGVGLAAPQIGLSQRLFVAVELRELV
cPDF       -MIRDLEYYDSPILRKVAAPVTEITDELRQLVLDMSETMAFYKGVGLAAPQVGQSISLFIMGVERELE
 _consrvd               **     *             *   *    * ** * *

 _aln.p   70         80         90        100        110        120        130
1RL4A      ----------RIFINPSIVEQSLVKLKLIEGCLSFPGIEGK-VERPSIVSISYYDINGYKHLKILKGI
1XEOA      -------DERLVLINPELLEKS-GETGIEEGCLSIPEQRAL-VPRAEKVKIRALDRDGKPFELEADGL
1N5NA      -------SEPRVFINPEFEPLTEEMDQYQEGCLSVPGFYEN-VDRPQKVRIKALDRDGNPFEEVAEGL
1V3YA      -------RRVYVVANPVITYRE-GLVEGTEG-LSLPGLYSEEVPRAERIRVEYQDEEGRGRVLELEGY
cPDF       DGELVFCDFPRVFINPVITQKSEQLVYGNEGCLSIPGLRGE-VARPDKITVSAKNLDGQQFSLALEGF
 _consrvd               **             ** ** *      * *            *        *

 _aln.pos  140        150        160        170        180
1RL4A      HSRIFQHEFDHLNGTLFIDKM-TQVDKKKVRPKLNELIRD-------
1XEOA      LAICIQHEMDHLVGKLFMDYL-S---PLKQQRIRQKVEKLD---RLK
1N5NA      LAVCIQHECDHLNGKLFVDYL-S---TLKRDRIRKKLEKQH---RQQ
1V3YA      MARVFQHEIDHLDGILFFERLPKPKREAFLEANRAELVRFQ---KEA
cPDF       LARIVMHETDHLHGVLYIDRMSDKDKTKQFKNNLEKIRRKYSILRGL
 _consrvd        ** *** * *
```

Figure 1 Multiple templates approach sequence alignment.

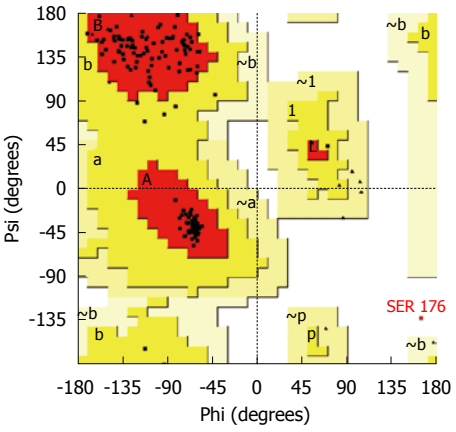

Figure 2 Ramachandran plot of model resulting from loop refinement of multiple template model.

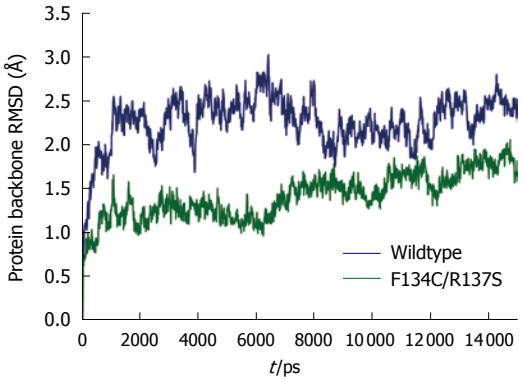

Figure 3 Molecular dynamics protein backbone atom root mean square deviation plot.

namics work. All bonds to hydrogen were restrained using the "shake" method[26]. A preliminary dynamics step restraining motion of the protein while gradually increasing temperature from 0 K to 300 K was run for 100 ps. This step was followed by a constant temperature (300 K) and constant pressure (1 bar) production run for a time period of 15 ns. As shown in Figure 3, at the end of this 15-ns period, the protein backbones of both wild-type cPDF and the F134C/R137S mutant had fully stabilized. Structural averages of the proteins were calculated from the last 3 ns of simulation and were refined using *in vacuo* energy minimization. The average per residue temperature factors were calculated from atomic root mean square fluctuation data obtained from the last 2 ns of simulation trajectory.

Construction and production of recombinant cPDF

A pET21-based expression vector for wild-type cPDF carrying a carboxyl terminal $(His)_6$-tag has been previously described[11]. This vector was used as the template for the construction of the D68R, E70R, D68R/E70R or ΔD68-V72 cPDF variants using a QuickChange site-directed mutagenesis kit (Stratagene). Sequence authenticity of the cPDF-coding sequence in the vectors was verified by automated DNA sequencing. Production and purification of the recombinant proteins were carried out following published procedures with modifications[11]. Plasmid-transformed ArcticExpress *E. coli* was cultured on a shaker at 30℃. When the A_{600} of the culture reached about 0.8, the culture temperature was lowered to 13℃, isopropyl β-D-1-thiogalactopyranoside (final concentration: 1 mmol/L) and $CoCl_2$ (final concentration: 100 μmol/L) were added to the culture to induce cPDF gene transcription and subsequent synthesis of cobalt-containing cPDF enzyme. After overnight culture at 13℃, the bacteria were collected by centrifugation, and lysed by a French Press. Cell debris was removed by centrifugation at 25000 *g* for 30 min. cPDFs were purified with the Talon affinity metal Agarose (Clontech) and stored at -80℃ after the addition

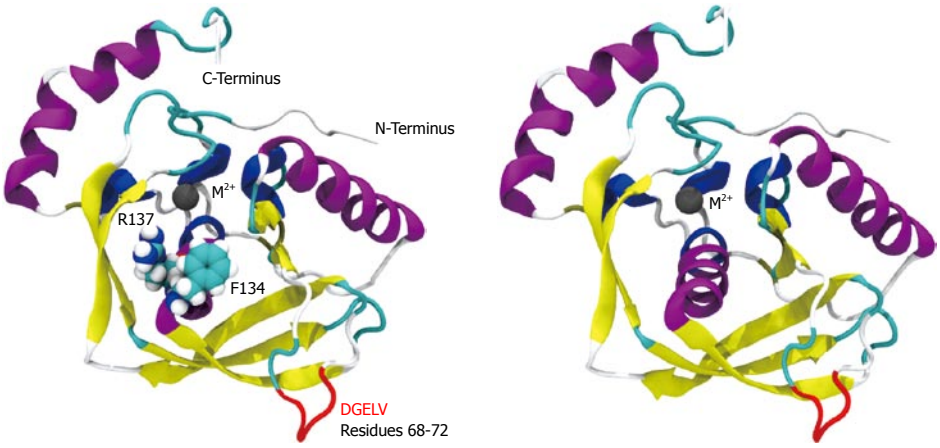

Figure 4 Cartoon depiction of wild-type structure showing Phe134 and Arg137 near the active site (left) and the "clean" overall structure model (right).

of glycerol to a final concentration of 10%.

PDF activity assay

An assay previously developed for the *E. coli* PDF[27] was modified to measure the activity of the chlamydial enzyme. The assay mix, in a total of 50 μL reaction volume, contained 50 mmol/L HEPES (pH 7.2), 10 mmol/L NaCl, 125 ng PDF, 0-50 mmol/L formyl-Met-Ala-Ser (fMAS) and 50-500 nmol/L GM6001. The deformylation reaction was allowed to proceed at 37℃ for 10 min and then terminated by heating at 95℃ for 2 min. The amount of MAS produced was reported by 2,4,6 trinitrobenzene sulfonic acid (TNBSA) that reacts with the free amine group to form a chromogenic peptide conjugate. Briefly, 550 μL of 0.0036% TNBSA, freshly prepared in 0.1 mol/L $NaHCO_3$, was added to the reaction and incubated at 37℃ for 1 h. Following the addition of 200 μL SDS and 100 μL 1.0 mol/L HCl, the peptide-TNBSA conjugate was quantified by measuring A_{335}. All A_{335} values were within the range of free methionine standards. Kinetic constants were calculated from the Lineweaver-Burk plots. Data presented are mean ± SD of three experiments.

RESULTS

Generation of a tertiary structural model for cPDF

We have previously demonstrated that chlamydiae are susceptible to hydroxamate-based metalloprotease inhibitors. By selecting and genome sequencing of the resistant mutants, we have identified cPDF as the target of the inhibitors[11]. One of the mutants has two nucleotide changes in the coding region, resulting in two amino acid substitutions (F134C and R137S) in the cPDF protein (observations from lab of Fan H to be published elsewhere). The mutant protein carrying a carboxyl terminal $(His)_6$-tag (i.e. F134C/R137S cPDF) was expressed in *E. coli* and purified to apparent homogeneity. Compared to wild-type cPDF, the F134C/R137S variant had a nearly 10-fold higher K_m when fMAS was used as a substrate, a sevenfold higher k_{cat}, a nearly 30% lower k_{cat}/K_m, and > 6-fold higher K_i for the inhibitor GM6001 (observations from lab of Fan H to be published elsewhere).

We conducted molecular simulation to understand how the amino acid sequence change affects enzyme catalysis. We first built a homology model of cPDF, because its experimental structure does not exist. The structures of PDFs from several other species are well known and were used to build the model of cPDF. A Ramachandran plot based on an analysis of 118 structures of resolution of at least 0.2 nm and R-factors no greater than 20% is shown in Figure 2. In the plot, 148 of the total 181 residues (93.1%) in cPDF were found in the most favored region, and 10 residues (6.3%) in an additional allowed region, and only one residue (0.6%), Ser176 at the C terminus, in a disallowed region. These data suggest that our model was of excellent quality because a good model requires only 90% of residues distributed in the most favored regions. According to our model, cPDF shares a conserved overall tertiary structure with the enzyme from other species studied (Figure 4), which is consistent with findings with other PDFs previously studied[5-8].

Increased atomic motion in a loop region of F134C/R137S cPDF

We computed the average temperature factor per residue for the protein backbone atoms to examine protein residue backbone mobility in the model. Temperature factor is an indicator of dynamic mobility, with higher factors indicating high mobility and low factors indicating low mobility. As shown in Figure 5, in addition to the anticipated high mobility at the C-terminal end, we also observed a significant amount of motion in a loop region spanning residues 61-76. Interestingly, the F134C/R137S cPDF showed a further sharp increase in the backbone atom motion in DGELV residues (68-72) within the loop (Figure 5), as compared to wild-type protein. The mutated residues 134 and 137 were located on a stable α helix forming the enzyme active site and their backbone atom motion remained stable and unaffected by mutations (Figure 4). These data suggest that amino acid substitutions at or near the active site of cPDF could alter the

Table 1 Effects of mutations in the DGELV loop region on catalytic properties

	Wild-type	D68R	E70R	D68R/E70R	Δ68-72
Km					
mM (mean ± SD)	6.8 ± 0.7	7.4 ± 1.2	6.1 ± 1.7	6.7 ± 0.4	18.6 ± 2.9
% control	100	109	91	99	275
kcat					
s^{-1} (mean ± SD)	37.9 ± 2.6	93.1 ± 8.4[b]	27.9 ± 4.3[a]	113.1 ± 10.9[b]	197.0 ± 29.0[b]
% control	100	246	74	299	520
kcat/Km					
$M^{-1}s^{-1}$ (mean ± SD)	5605 ± 357	12764 ± 970[b]	4652 ± 677	16781 ± 678[b]	10605 ± 301[b]
% control	100	228	83	299	189

[a]$P < 0.05$, [b]$P < 0.01$ (2-tailed Student *t* test for comparison with the wild-type chlamydial peptide deformylase).

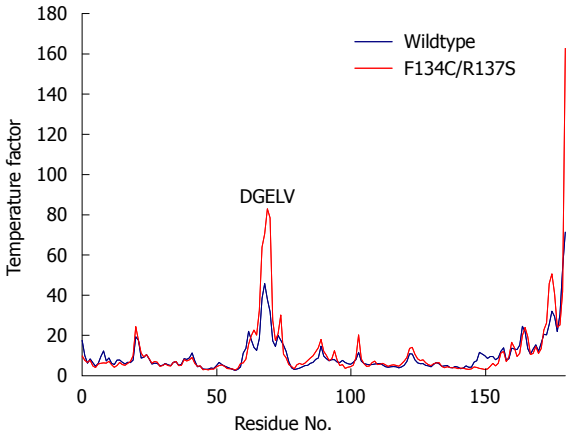

Figure 5. Increased atomic motion in loop residues Asp68 through Val72 (DGELV) in the F134C/R137S chlamydial peptide deformylase as reflected by average per residue backbone atom temperature factor.

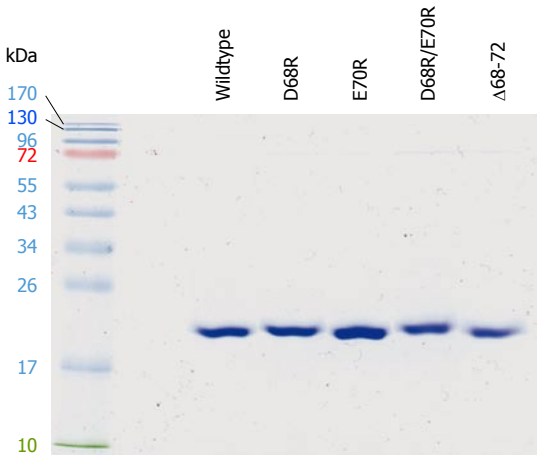

Figure 6 Purified recombinant chlamydial peptide deformylase proteins. Chlamydial peptide deformylases carrying a (His)$_6$-tag were expressed in *Escherichia coli,* purified by cobalt agarose, resolved by 13.5% SDS-polyacrylamide gel, and visualized by Coomassie blue staining. In the left lane are protein standards with molecular weights indicated.

stability of the loop region.

Sequence flexibility of the DGELV loop sequence

It has previously been demonstrated that mutation of any of three consecutive Asp residues to Lys in a loop region in mPDF, which corresponds to the loop region containing the DGELV sequence in cPDF, causes moderate decreases to severe loses in the enzyme activity[9,28]. Molecular simulation indicates structural changes in the substrate-binding pocket in the loop-mutated mPDF enzymes[9]. The mPDF study and our prediction of increased motion in the catalytically inefficient F134C/R137S cPDF prompted us to hypothesize that there may also be interdependence between the active site and the loop region in cPDF.

To test this hypothesis, we performed site-directed mutagenesis in the DGELV region of cPDF on the basis of a pET21 expression vector[11]. Thus, the negatively charged Asp68 and Glu70 residues were mutated, individually or in combination, to the positively charged Arg. Furthermore, a cPDF variant with the deletion of the DGELV sequence was also constructed. The cPDF variants as well as wild-type cPDF were expressed in *E. coli* and purified to apparent near homogeneity for kinetic analyses. A Coomassie-blue-stained gel with purified recombinant loop variants as well as the wild-type cPDF protein is shown in Figure 6. The K_m values of D68R, E70R and D68R/E70R cPDF were very similar to that of the wild-type enzyme (Table 1). Both the D68R and D68R/E70R variants exhibited significantly higher levels of k_{cat} and k_{cat}/K_m, whereas the D70E cPDF displayed a relatively small but statistically significant 26% decrease in k_{cat}, and an even smaller and statistically insignificant 17% drop in k_{cat}/K_m (Table 1). Compared to the wild-type enzyme, Δ68-72 cPDF had a fivefold higher k_{cat} and a twofold higher k_{cat}/K_m, although these were accompanied by a nearly threefold increase in K_m (Table 1). These data suggest that the cPDF enzyme is highly tolerant to radical mutations in the loop region.

Direct impact of F134C and R137S mutations on the loop

To understand how the atomic motion in the DGELV loop region is increased in the F134C/R137S cPDF variant, we examined the effect of the two amino acid substitutions on the structure of the enzyme. Our structural model showed that the combination of the two residue mutations led to an increase in space for the loop region to occupy. The R137S mutation broke the salt-bridge

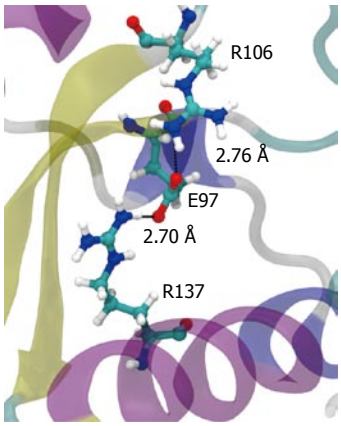

Figure 7 The salt-bridge "sandwich" in the wild-type. Residues Arg137, Glu97 and Arg106 form a tight salt bridge adding rigidity to the structure in the active site region. When broken, Arg106 is pulled more tightly into the active site.

Figure 8 Least squares fit of wild-type with F134C/R137S mutant backbone atoms. The wild-type is colored blue and the mutant red. Note shift of residue range Glu63 to Glu67 in the large loop region by 0.29 nm towards the active site. The overall average RMSD fit for the protein backbone atoms was 0.15 nm.

"sandwich" of Arg137-Glu97-Arg106 in the wild-type (Figure 7). The mutations caused Glu97 to shift over to the vacated space and brought Arg106 more tightly into the active site, which freed up space already made available by the F134C mutation in proximity to the loop (Figure 4). This resulted in the Glu63 to Glu67 region of the loop shifting towards the active site by 0.29 nm. This shift allowed for a higher degree of motion in the DGELV region in the F134C/R137S cPDF (Figure 8). Accordingly, there was an increase in atomic temperature factor in the dynamics simulation of the mutant (Figure 5).

DISCUSSION

A loop region in the mPDF has been shown to be critical for enzyme activity[9,28]. Accordingly, that enzyme has an extremely low level of tolerance to mutation of three consecutive Arg residues in this region. For one of the Arg residues, even a conserved Arg→Lys mutation results in severe loss of enzyme activity[9]. However, how important the corresponding loop is in other PDFs has not been examined. The increase in atomic motion in the DGELV region of the F134C/R137S mutant prompted us to assess the role of the equivalent cPDF loop region in enzyme function. Kinetic analyses showed that, in contrast to the mPDF, the cPDF tolerated radical mutations individually or in combination at Asp68 and Glu70. In fact, the single D68R and double D68R/E70R mutants appeared to be more efficient enzymes than wild-type cPDF, as indicated by significantly increased k_{cat} and k_{cat}/K_m values in the mutants. Clearly, cPDF has a high degree of sequence flexibility in the DGELV loop region. However, the observed kinetic changes in the loop mutants, together with the increased mobility of the DGELV region of the loop in the active site F134C/R137S mutant, do suggest that movement of this loop is involved in a rate-limiting conformational change of the enzyme during catalysis. Furthermore, our data do not exclude the possibility that the cPDF has more stringent sequence requirements in other regions of the loop.

It is particularly interesting why nature has not selected better enzymes such as the D68E mutant during evolution. Perhaps this is because the PDF enzyme activity needs to be controlled at the organismal level, as is the case with many other enzymes and proteins. Although peptide deformylation is required, it is not known what adverse effects too much PDF activity may have. Interestingly, the chlamydial vacuole of GR10, a cPDF-overexpressing mutant[11], has different morphology, compared to that of the parental strain. The mutant appears to generate a large aberrant replicating form (unpublished observations). cPDF is the only gene with a mutation in that mutant (unpublished observations from lab of Fan H), therefore, the abnormal morphology must have resulted from cPDF overexpression. Characterization of such aberrant structures will be useful to the understanding of a possible need for maintaining PDF activity at an appropriate level in normal chlamydial physiology, and perhaps, in general bacterial physiology as well.

Massive bacteria-based overexpression systems may result in incompletely deformylated proteins. This problem can be alleviated by PDF co-expression[29]. Owing to its higher catalytic efficiency, the D68R/E70R cPDF variant would be particularly useful if such a situation of incomplete deformylation of target protein arises, especially if the target protein is a chlamydial protein.

COMMENTS

Background

By removing the formyl group from the leading Met of newly synthesized proteins, peptide deformylase (PDF) is an essential enzyme for protein maturation in bacteria. PDF is a promising therapeutic target for infectious diseases including sexually transmitted infection caused by *Chlamydia trachomatis*. It has recently been discovered that substitution of two amino acids near the active site of the chlamydial PDF (cPDF) contributes to resistance.

Research frontiers

Characterization of individual PDFs is of significance for the development of narrow-spectrum PDF inhibitors that target specific pathogens. Elucidation of resistance mechanisms may provide invaluable information for the design of

new inhibitors with improved targeting efficacy.

Innovations and breakthroughs

By combining simulation, site-directed mutagenesis and kinetic analysis, this study revealed a role of the DGELV loop region in the catalysis and inhibition efficiency in cPDF, and a remarkably high level of tolerance to radical mutations in the loop region. It is believed that this is the only study that has examined the role of the loop in catalysis by the PDF enzyme, besides the mycobacterial PDF (mPDF). The sequence flexibility in cPDF is in striking contrast to that of mPDF.

Applications

The findings presented in this report have implications for the development of PDF-inhibitor-based antibacterials, including those for chlamydial infection and tuberculosis. The cPDF variants with increased catalytic efficiency may be useful for heterologous protein expression requiring improved *N*-deformylation efficiency.

Terminology

Temperature factor is an indicator of dynamic mobility. Higher factors indicate high mobility and low factors indicate low mobility.

Peer review

In this study, Oey *et al* studied the function of a loop region in cPDF using molecular modeling and biochemical analysis. This work is related to the development of new anti-infective agents, a topic that is both timely and important. The introduction is well presented. The methods are adequate and vigorous. Data are robust and properly discussed. Additional references for the nature of current PDF inhibitors should be provided; as should data documenting the purity of recombinant cPDFs.

REFERENCES

1 **Tobias JW**, Shrader TE, Rocap G, Varshavsky A. The N-end rule in bacteria. *Science* 1991; **254**: 1374-1377

2 **Sharma A**, Khuller GK, Sharma S. Peptide deformylase--a promising therapeutic target for tuberculosis and antibacterial drug discovery. *Expert Opin Ther Targets* 2009; **13**: 753-765

3 **Chen D**, Yuan Z. Therapeutic potential of peptide deformylase inhibitors. *Expert Opin Investig Drugs* 2005; **14**: 1107-1116

4 **Leeds JA**, Dean CR. Peptide deformylase as an antibacterial target: a critical assessment. *Curr Opin Pharmacol* 2006; **6**: 445-452

5 **Chan MK**, Gong W, Rajagopalan PT, Hao B, Tsai CM, Pei D. Crystal structure of the Escherichia coli peptide deformylase. *Biochemistry* 1997; **36**: 13904-13909

6 **Kreusch A**, Spraggon G, Lee CC, Klock H, McMullan D, Ng K, Shin T, Vincent J, Warner I, Ericson C, Lesley SA. Structure analysis of peptide deformylases from Streptococcus pneumoniae, Staphylococcus aureus, Thermotoga maritima and Pseudomonas aeruginosa: snapshots of the oxygen sensitivity of peptide deformylase. *J Mol Biol* 2003; **330**: 309-321

7 **Dirk LM**, Schmidt JJ, Cai Y, Barnes JC, Hanger KM, Nayak NR, Williams MA, Grossman RB, Houtz RL, Rodgers DW. Insights into the substrate specificity of plant peptide deformylase, an essential enzyme with potential for the development of novel biotechnology applications in agriculture. *Biochem J* 2008; **413**: 417-427

8 **Cai J**, Han C, Hu T, Zhang J, Wu D, Wang F, Liu Y, Ding J, Chen K, Yue J, Shen X, Jiang H. Peptide deformylase is a potential target for anti-Helicobacter pylori drugs: reverse docking, enzymatic assay, and X-ray crystallography validation. *Protein Sci* 2006; **15**: 2071-2081

9 **Saxena R**, Kanudia P, Datt M, Dar HH, Karthikeyan S, Singh B, Chakraborti PK. Three consecutive arginines are important for the mycobacterial peptide deformylase enzyme activity. *J Biol Chem* 2008; **283**: 23754-23764

10 **Schachter J**. Infection and disease epidemiology. In: Stephens RS, editor. Chlamydia: intracellular biology, pathogenesis, and immunity. Washington DC: ASM Press, 1999: 139-169

11 **Balakrishnan A**, Patel B, Sieber SA, Chen D, Pachikara N, Zhong G, Cravatt BF, Fan H. Metalloprotease inhibitors GM6001 and TAPI-0 inhibit the obligate intracellular human pathogen Chlamydia trachomatis by targeting peptide deformylase of the bacterium. *J Biol Chem* 2006; **281**: 16691-16699

12 **Balakrishnan A**, Wang L, Li X, Ohman-Strickland P, Malatesta P, Fan H. Inhibition of chlamydial infection in the genital tract of female mice by topical application of a peptide deformylase inhibitor. *Microbiol Res* 2009; **164**: 338-346

13 **Humphrey W**, Dalke A, Schulten K. VMD: visual molecular dynamics. *J Mol Graph* 1996; **14**: 33-38, 27-28

14 **Eswar N**, Webb B, Marti-Renom MA, Madhusudhan MS, Eramian D, Shen MY, Pieper U, Sali A. Comparative protein structure modeling using Modeller. *Curr Protoc Bioinformatics* 2006; **Chapter 5**: Unit 5.6

15 **Robien MA**, Nguyen KT, Kumar A, Hirsh I, Turley S, Pei D, Hol WG. An improved crystal form of Plasmodium falciparum peptide deformylase. *Protein Sci* 2004; **13**: 1155-1163

16 **Jain R**, Hao B, Liu RP, Chan MK. Structures of E. coli peptide deformylase bound to formate: insight into the preference for Fe2+ over Zn2+ as the active site metal. *J Am Chem Soc* 2005; **127**: 4558-4559

17 **Kamo M**, Kudo N, Lee WC, Motoshima H, Tanokura M. Crystallization and preliminary X-ray crystallographic analysis of peptide deformylase from Thermus thermophilus HB8. *Acta Crystallogr D Biol Crystallogr* 2004; **60**: 1299-1300

18 **Laskowski RA**, MacArthur MW, Moss DS, Thornton JM. PROCHECK: a program to check the stereochemical quality of protein structures. *J Appl Cryst* 1993; **26**: 283-291

19 **Case DA**, Cheatham TE, Darden T, Gohlke H, Luo R, Merz KM, Onufriev A, Simmerling C, Wang B, Woods RJ. The Amber biomolecular simulation programs. *J Comput Chem* 2005; **26**: 1668-1688

20 **Duan Y**, Wu C, Chowdhury S, Lee MC, Xiong G, Zhang W, Yang R, Cieplak P, Luo R, Lee T, Caldwell J, Wang J, Kollman P. A point-charge force field for molecular mechanics simulations of proteins based on condensed-phase quantum mechanical calculations. *J Comput Chem* 2003; **24**: 1999-2012

21 **Pang YP**, Xu K, Yazal JE, Prendergas FG. Successful molecular dynamics simulation of the zinc-bound farnesyltransferase using the cationic dummy atom approach. *Protein Sci* 2000; **9**: 1857-1865

22 **Pérez L**, Kerrigan JE, Li X, Fan H. Substitution of methionine 435 with leucine, isoleucine, and serine in tumor necrosis factor alpha converting enzyme inactivates ectodomain shedding activity. *Biochem Cell Biol* 2007; **85**: 141-149

23 **Berendsen HJC**, Grigera JR, Straatsma TP. The missing term in effective pair potentials. *J Phys Chem* 1987; **91**: 6269-6271

24 **Darden T**, York D, Pedersen L. Particle mesh Ewald: An N . log(N) method for Ewald sums in large systems. *J Chem Phys* 1993; **98**: 10089-10092

25 **Essmann U**, Perera L, Berkowitz ML, Darden T, Lee H, Pedersen LG. A smooth particle mesh ewald potential. *J Chem Phys* 1995; **103**: 8577-8592

26 **Miyamoto S**, Kollman PA. Settle: An analytical version of the SHAKE and RATTLE algorithm for rigid water models. *J Comp Chem* 1992; **13**: 952-962

27 **Groche D**, Becker A, Schlichting I, Kabsch W, Schultz S, Wagner AF. Isolation and crystallization of functionally competent Escherichia coli peptide deformylase forms containing either iron or nickel in the active site. *Biochem Biophys Res Commun* 1998; **246**: 342-346

28 **Saxena R**, Chakraborti PK. Identification of regions involved in enzymatic stability of peptide deformylase of Mycobacterium tuberculosis. *J Bacteriol* 2005; **187**: 8216-8220
29 **Warren WC**, Bentle KA, Schlittler MR, Schwane AC, O'Neil JP, Bogosian G. Increased production of peptide deformylase eliminates retention of formylmethionine in bovine somatotropin overproduced in Escherichia coli. *Gene* 1996; **174**: 235-238

S- Editor Cheng JX **L- Editor** Kerr C **E- Editor** Zheng XM